



# Meiocyte Isolation by INTACT and Meiotic Transcriptome Analysis in *Arabidopsis*

Lucia Barra<sup>1†</sup>, Pasquale Termolino<sup>1†</sup>, Riccardo Aiese Cigliano<sup>2†</sup>, Gaetana Cremona<sup>1</sup>, Rosa Paparo<sup>1</sup>, Carmine Lanzillo<sup>1</sup>, Maria Federica Consiglio<sup>1</sup> and Clara Conicella<sup>1\*</sup>

<sup>1</sup> Institute of Biosciences and Bioresources, National Research Council of Italy, Portici, Italy, <sup>2</sup> Sequentia Biotech SL, Barcelona, Spain

## OPEN ACCESS

### Edited by:

Olivier Da Ines,  
Université Clermont Auvergne, France

### Reviewed by:

Wei-Hua Tang,  
Shanghai Institutes for Biological  
Sciences (CAS), China  
Josh T. Cuperus,  
University of Washington,  
United States

### \*Correspondence:

Clara Conicella  
conicell@unina.it

†These authors have contributed  
equally to this work and share first  
authorship

### Specialty section:

This article was submitted to  
Plant Cell Biology,  
a section of the journal  
Frontiers in Plant Science

Received: 04 December 2020

Accepted: 01 February 2021

Published: 04 March 2021

### Citation:

Barra L, Termolino P,  
Aiese Cigliano R, Cremona G,  
Paparo R, Lanzillo C, Consiglio MF  
and Conicella C (2021) Meiocyte  
Isolation by INTACT and Meiotic  
Transcriptome Analysis  
in *Arabidopsis*.  
Front. Plant Sci. 12:638051.  
doi: 10.3389/fpls.2021.638051

Isolation of nuclei tagged in specific cell types (INTACT) is a method developed to isolate cell-type-specific nuclei that are tagged through *in vivo* biotin labeling of a nuclear targeting fusion (NTF) protein. In our work, INTACT was used to capture nuclei of meiocytes and to generate a meiotic transcriptome in *Arabidopsis*. Using the promoter of *AtDMC1* recombinase to label meiotic nuclei, we generated transgenic plants carrying *AtDMC1:NTF* along with biotin ligase enzyme (*BirA*) under the constitutive *ACTIN2* (*ACT2*) promoter. *AtDMC1*-driven expression of biotin-labeled *NTF* allowed us to collect nuclei of meiocytes by streptavidin-coated magnetic beads. The nuclear meiotic transcriptome was obtained by RNA-seq using low-quantity input RNA. Transcripts grouped into different categories according to their expression levels were investigated by gene ontology enrichment analysis (GOEA). The most enriched GO term “DNA demethylation” in mid/high-expression classes suggests that this biological process is particularly relevant to meiosis onset. The majority of genes with established roles in meiosis were distributed in the classes of mid/high and high expression. Meiotic transcriptome was compared with public available transcriptomes from other tissues in *Arabidopsis*. Bioinformatics analysis by expression network identified a core of more than 1,500 genes related to meiosis landmarks.

**Keywords:** meiosis, meiocyte, tagged nuclei, RNA-seq, meiotic transcriptome

## INTRODUCTION

Meiosis is a complex process critical to sexual reproduction. In plants, meiosis appears to be influenced by environmental cues (reviewed in De Storme and Geelen, 2014; Si et al., 2015). Within this context, global climate change is expected to have an impact on crop production with consequences for food security (Parry et al., 1999). To face the new challenges, a fundamental understanding of meiosis is required in model, crop, and non-model plants (Lambing and Heckmann, 2018). Molecular knowledge of plant meiosis has primarily advanced through understanding the function of single genes involved in key steps being benefited by the conserved pathways across model species (reviewed in Mercier et al., 2015). Thereafter, transcriptome studies of specific cell types improved our understanding of the gene-expression landscape during meiosis (reviewed in Dubowicz-Shulze and Chen, 2014). However, the isolation of plant meiocytes is challenging due to the difficulty in accessing the germline cells. Pollen mother cells and embryo

sac mother cells are enclosed by sporophytic tissues, i.e., anthers and ovules inside the flower buds. Over the last decade, different techniques were established for targeted isolation of meiocytes by micromanipulation (Chen et al., 2010; Libeau et al., 2011; Yang et al., 2011; Nelms and Walbot, 2019) and laser microdissection (Tang et al., 2010; Schmidt et al., 2011; Barra et al., 2012; Yuan et al., 2018).

An alternative method that achieves the isolation of nuclei tagged in specific cell types (INTACT) was developed by Deal and Henikoff (2011). INTACT overcomes the limitation of time-consuming manual dissection generally associated with contamination of undesired cells. Therefore, INTACT allows rapid and efficient nucleus isolation with the advantage of not requiring specialized and expensive equipment (Deal and Henikoff, 2010). INTACT is based on *in vivo* biotin labeling of a nuclear targeting fusion (NTF) protein which consists of three parts corresponding to (1) a unique target peptide of biotin ligase recognition (BLRP), (2) a domain from *Arabidopsis* RAN GTPASE ACTIVATING PROTEIN 1 (RanGAP1) for nuclear envelope localization (Rose and Meier, 2001), and (3) green fluorescent protein (GFP) for visualization. BLRP acts as a substrate for the BirA biotin ligase enzyme from *Escherichia coli* (Beckett et al., 1999). *BirA* and *NTF* need to be co-expressed in the same cell.

So far, INTACT has been used in combination with transcriptomic, epigenomic, and proteomic studies in different species including plants (Amin et al., 2014; Agrawal et al., 2019; Del Toro-De León and Köhler, 2019). However, in plants, a broad use of INTACT across different cell types remains challenging since it requires a cell-type marker and a method for genetic transformation for the species of interest. A peculiarity of INTACT is that it provides nuclear RNAs which could differ from cytosolic RNAs depending on the selective compartment enrichment of RNAs influenced by mechanisms such as nuclear retention and posttranscriptional regulation (Reynoso et al., 2018). For instance, the comparison between nuclear and total RNAs furnished additional insights into the transcriptome regulation in the early *Arabidopsis* embryo (Palovaara et al., 2017). In the future, INTACT could contribute to the elucidation of the transcriptome reorganization occurring in meiosis, particularly at the prophase I expression transitions that were recently defined in maize by single-cell RNA sequencing (Nelms and Walbot, 2019).

In this work, we applied the INTACT-based approach to obtain purified meiocyte nuclei from the total cell pool of floral bud in *Arabidopsis thaliana*. To label meiotic nuclei, we used the promoter of *AtDMC1* recombinase (Klimyuk and Jones, 1997; De Muyt et al., 2009). The *AtDMC1*-driven expression of biotin-labeled NTF allowed us to isolate meiocyte nuclei using streptavidin-coated magnetic beads. The meiotic nuclear transcriptome was obtained by RNA-seq and validated through analysis of the expression of known meiotic genes and the comparison with other tissues. Finally, expression network analysis was performed to find new candidate genes involved in the meiotic process.

## MATERIALS AND METHODS

### Plant Material, Transformation, and Growth Conditions

The transgenic line expressing *ACT2:BirA*, kindly given by Prof. R. Deal (Emory University, United States), and the reference ecotype Col-0 of *A. thaliana* (NASC stock N60000) were used in this work. The transgenic line was transformed by *Agrobacterium tumefaciens* (GV3101) according to floral dip method (Clough and Bent, 1998) to obtain plants carrying *DMC1:NTF* along with *ACT2:BirA*. About 1,500 seeds obtained after transformation were sterilized with 70% ethanol for 1 min., and bleach solution (10% commercial bleach and 0.05% Tween 20) for 10 min., finally washed with sterile water three times. Sterilized seeds were sown on a selective modified MS (Murashige and Skoog, 1962) medium containing hygromycin (50 mg/l) and 0.8% agar, kept for 2–3 days at 4°C, and germinated under long-day conditions (16 h light/8 h darkness) at 24°C. Seedlings transferred to pots were grown in a controlled growth chamber under long-day conditions. The *ADMCI:NTF/ACT2:BirA* double homozygous transgenic line (D.1) was selected from ten T<sub>2</sub> independent transformant lines. About 200 plants from the D.1 line were grown as above reported for subsequent experiments.

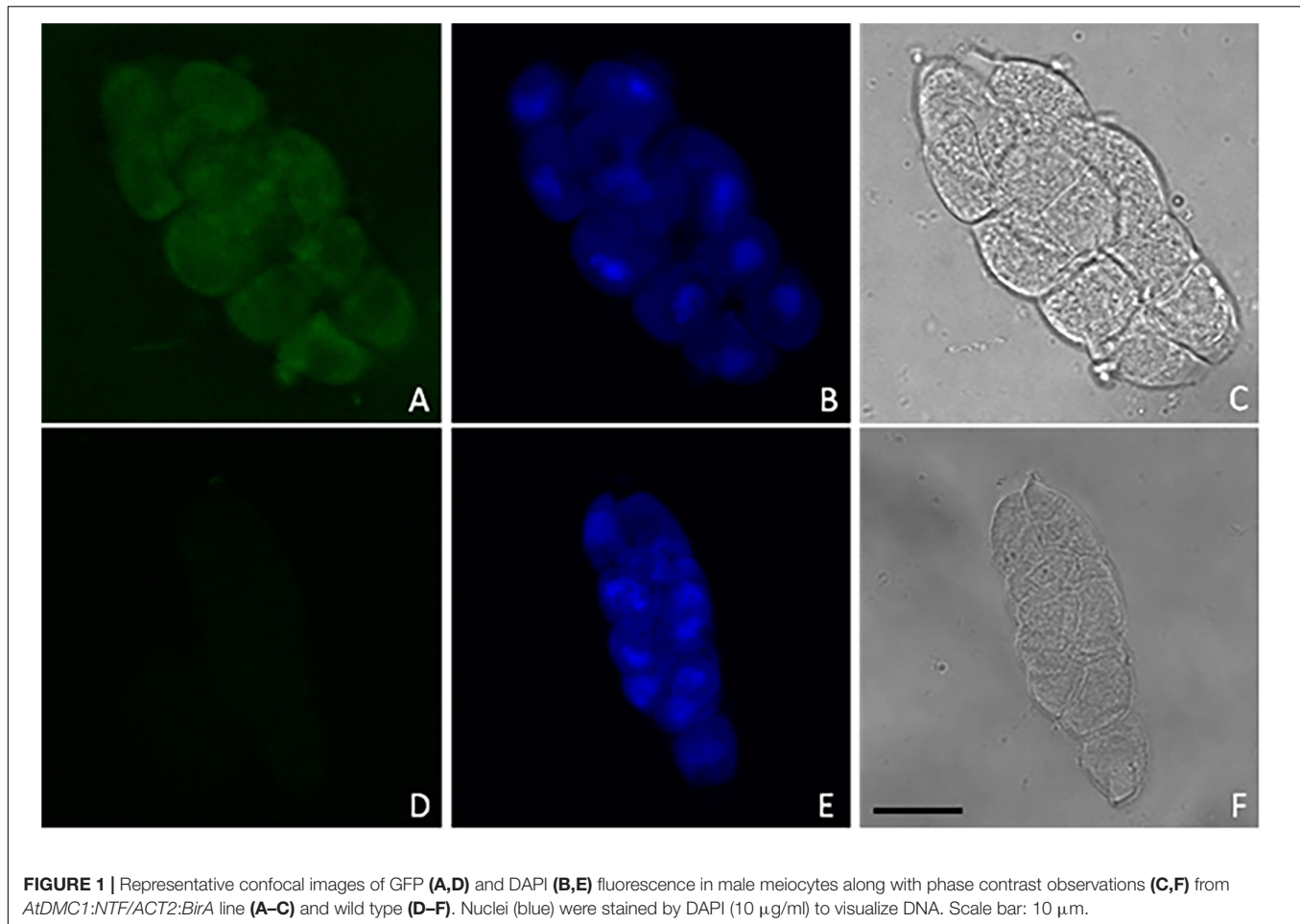
### PCR and RT-qPCR

To confirm transgene insertion, PCR was conducted on the hygromycin resistance gene used as a selectable marker. Genomic DNA was extracted from leaf tissue of transgenic plants using the DNeasy Plant Mini Kit (Qiagen)<sup>1</sup> according to the manufacturer's instructions. PCR reactions were performed on genomic DNA using primers listed in **Supplementary Table 1**. RT-qPCR was performed to verify expression of target *BirA* gene under the constitutive promoter *ACT2* in the floral buds. Total RNA from transgenic *ACT2:BirA* plants was extracted using RNeasy plant minikit (QIAGEN) following the manufacturer's instructions. mRNA was retrotranscribed to cDNA using Superscript III reverse transcriptase (Thermo Fisher Scientific, United States) and oligo dT(20) following the manufacturer's conditions, and relative expression was verified by real-time qPCR. The experiment was performed on a QIAGEN Rotorgene 6,000 qRT-PCR machine, using Power Sybr Green real time mix (Thermo Fisher Scientific, United States). The reaction conditions were as follows: one cycle at 95°C for 10 min, and 40 cycles of 95°C × 10'' denaturation and 60°C × 45'' annealing and extension. The melting curve was run to verify the specificity of the primers. The *ADENINE PHOSPHORIBOSYL TRANSFERASE 1 (APT1)* gene was used as a housekeeping internal control. Target and housekeeping primers are listed in **Supplementary Table 2**.

### Construct for INTACT, Nucleus Isolation, and Microscopy

The fusion gene *NTF* carried in the vector ADF8-NTF, kindly given by Prof. R. Deal (Emory University, United States),

<sup>1</sup><https://www.qiagen.com/>



and the *AtDMC1* promoter carried in the vector SLJ7753, kindly given by Prof. J.D.G. Jones (The Sainsbury Laboratory, Norwich, United Kingdom), were amplified with specific primers carrying GATEWAY adapters. Subsequently, they were cloned into Gateway vectors pDONR/Zeo and pDONR/P4P1R, respectively (Thermo Fisher Scientific). Generated entry clones were recombined with multisite GATEWAY reaction into destination vector pH7m24GW,<sup>2</sup> and the final expression clone, named pEXPR-DMC1-NTF, was generated. All gateway reactions were performed following the manufacturer's standard protocols. Primers used for vector construction are listed in **Supplementary Table 3**.

Flower buds of the size corresponding to male meiotic stage (Smyth et al., 1990) were collected, fixed with 1% formaldehyde solution, and stored at  $-80^{\circ}\text{C}$ . Nuclei were purified from 1.5 g of frozen and homogenized tissue as described previously by Wang and Deal (2015) with some minor modifications. In particular, the tissue immersed in 40 ml of Nuclei Purification Buffer solution (NPBF) containing 20 mM MOPS (pH 7), 40 mM NaCl, 90 mM KCl, 2 mM EDTA, 0.5 mM EGTA, 0.5 mM spermidine, 0.2 mM spermine, 1% (v/v) formaldehyde was incubated in 50 ml tube under vacuum glass desiccator for 10 min., and

vacuum release for 2 min. The procedure was repeated once. Then, glycine was added to a final concentration of 0.125 M under vacuum for 7 min. After NPBF solution elimination, the tissue was washed three times with water. Isolated nuclei were resuspended into RNAlater buffer, and RNA extraction was performed immediately.

Laser-scanning confocal microscopy imaging was performed using a confocal Zeiss LSM 510. Isolated nuclei were observed using a Fluorescence Microscope (Leitz Aristoplan).

### RNA Extraction and Sequencing

Total RNA was extracted from three replicates of isolated nuclei using an RNeasy Extraction Mini Kit (Qiagen, see text footnote 1) according to the manufacturer's instructions. Isolated nuclei derived from the same population of inflorescences where the buds different from stage 9 (Smyth et al., 1990) had been manually dissected. Quantification was performed on a QUBIT fluorometer.

RNA sequencing was performed by IGA Technology Services Srl<sup>3</sup>. The libraries were produced using retrotranscribed cDNA previously amplified by Ovation Ultralow Library System V2 (NuGEN Technologies, Inc.). Library size and integrity were

<sup>2</sup><https://gateway.psb.ugent.be/search>

<sup>3</sup>[appliedgenomics.org](http://appliedgenomics.org)

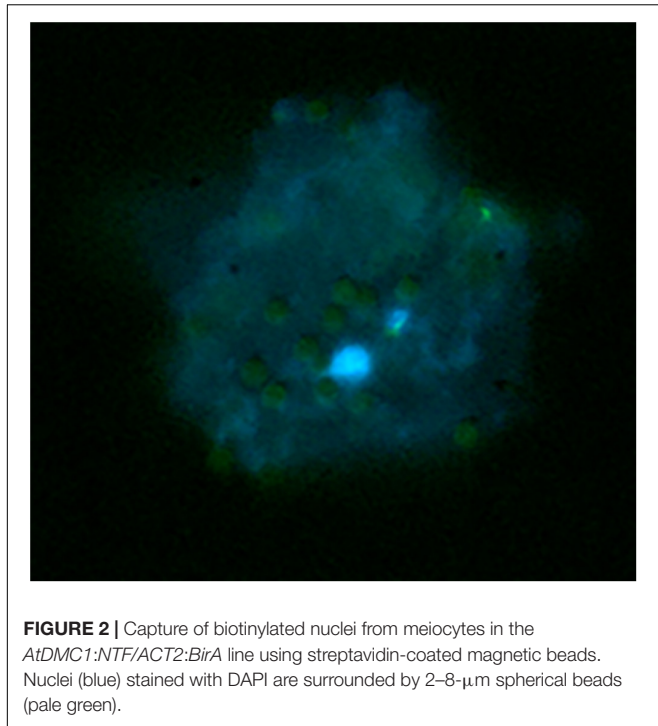


**FIGURE 2** | Capture of biotinylated nuclei from meiocytes in the *AtDMC1:NTF/ACT2:BirA* line using streptavidin-coated magnetic beads. Nuclei (blue) stained with DAPI are surrounded by 2–8- $\mu\text{m}$  spherical beads (pale green).

assessed using the Agilent Bioanalyzer (Santa Clara, CA) or Caliper GX (PerkinElmer, MA). Sequencing was performed by Illumina HiSeq 2,500 (Illumina, San Diego, CA) and 30-M paired-end reads ( $2 \times 125$ ) per replicate were generated.

## Bioinformatics

Raw sequencing data (FASTQ files) were quality checked using the software FASTQC v0.11.5<sup>4</sup>, then low-quality bases and adapter sequences were removed with the software BBDuk v35 (Bushnell et al., 2017) setting 35 bp as the minimum read length after trimming. The read length ranged from 35 to 125 bp after trimming. More than 98% of the final reads had a length of 125 bp since adapter contamination was very low. The trimmed reads were then mapped against the *A. thaliana* reference genome (Araport11) (Cheng et al., 2016) using STAR v2.7.3a with the option –alignEndsProtrude 100 DiscordantPair. The statistics from the mapping step were produced with Qualimap v2.2.1 (Okonechnikov et al., 2016). Kallisto v0.46.0 was used to obtain transcript expression quantification levels, as estimated counts and TPMs, which were then summarized as gene expression values using the R package “tximport” (Soneson et al., 2016).

The correlation analysis of the samples was performed using the R in-built function “cor,” and the results were plotted with the function “corrplot.” The classification of the gene classes and the saturation analysis were performed with the R package “NOISeq” (Tarazona et al., 2015). Genes were classified based on their average expression levels using the following criteria: “undetected” if the expression was 0 across all the replicates, “Low” if  $\log_2$  average TPM  $\leq 1.252$ , “Low\_Mid”

if  $\log_2$  average TPM  $> 1.252$  and  $\leq 2.207$ , “Mid\_High” if  $\log_2$  average TPM  $> 2.207$  and  $\leq 4.169$ , and “High” if  $\log_2$  average TPM  $> 4.169$ . The abovementioned values correspond to the 25th, 50th, and 75th percentiles of the  $\log_2$  average TPM distributions, respectively.

In order to compare the expression profile of the meiocytes against other datasets, TPM values from the following datasets were downloaded from EBI: E-GEOD-38612, E-GEOD-55866, and E-MTAB-4202 (Supplementary Table 4). In addition, gene expression profiles from pollen and tapetum cells were obtained from Loraine et al. (2013) and Li et al. (2017). When multiple replicates of the same tissue were available, an average was calculated. Similarly, when multiple developmental stages of the same tissue were available, the average was calculated. The only exception consisted of the tapetum datasets kept separate because the two available stages were highly different. Finally, a complete expression matrix was obtained by merging all the datasets and the ARSyN function from the NOISeq package was used to remove the batch effect. A PCA analysis was then performed with the in-built “prcomp” function in R and the results plotted with “ggplot2.”

A gene expression network was generated using the expression matrix obtained after the ARSyN correction, following the Aracne algorithm implemented in the R package “parmigene” (Sales and Romualdi, 2011). Cytoscape v3.8.1 was then used to plot the network and select only the first neighbors of known meiotic genes in order to find new candidates. The gene ontology (GO) analysis of the obtained genes was then performed using the Cytoscape app named “BinGO” using the hypergeometric test as a statistical test and an FDR lower than 0.05 as threshold. All the heat maps were generated using Clustvis (Metsalu and Vilo, 2015).

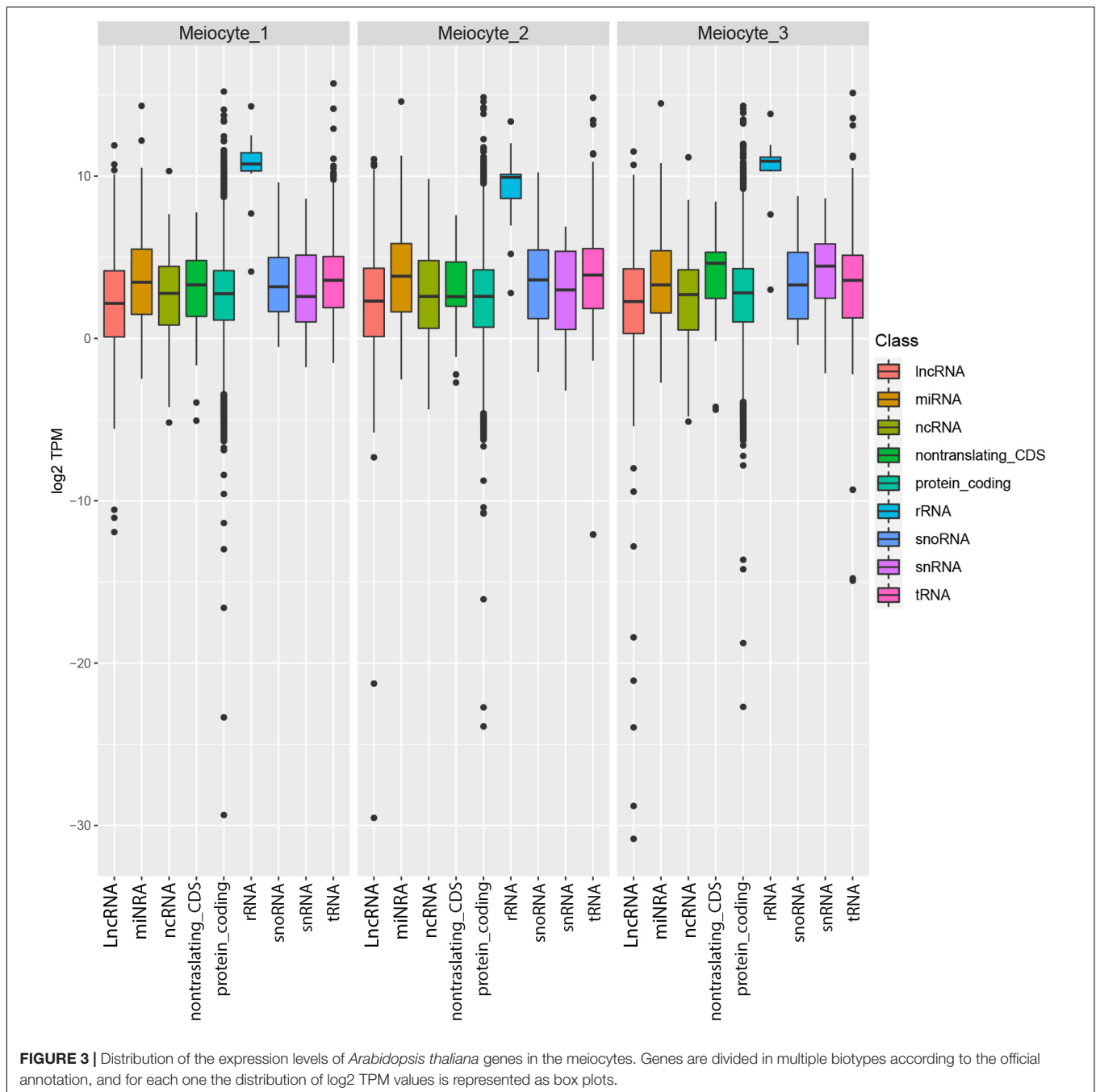
Gene ontology enrichment analysis (GOEA) were performed using in-house scripts based on the method described in Tian et al. (2017) and setting a minimum FDR threshold of 0.05.

## RESULTS

### Generation of Transgenic Material and Isolation of Nuclei From Meiocytes Using INTACT in Arabidopsis

In order to isolate meiocyte nuclei by the INTACT method for RNA-seq analysis in Arabidopsis, we generated transgenic material carrying a *NTF* protein under the meiosis-specific *AtDMC1* promoter (Klimyuk and Jones, 1997) along with the biotinylase *BirA* under a constitutive *ACTIN2* (*ACT2*) promoter. The promoter of *ACT2* (At3g18780) was used by Deal and Henikoff (2011) to drive expression of *BirA* in root cell types (An et al., 1996). Following detection of *ACT2:BirA* expression in floral buds (not shown), we used the same transgenic line generated by Deal and Henikoff (2011) as starting material. In this line, we introduced the new construct carrying the *AtDMC1:NTF* expression cassette. Although *AtDMC1* (At3g22880) was expected to drive *NTF* expression in both male and female meiocytes (Klimyuk and Jones, 1997), we restricted

<sup>4</sup><https://www.bioinformatics.babraham.ac.uk/projects/fastqc/>



our confocal microscopy analysis to anthers and male meiocytes. Indeed, the flower buds were collected at a stage corresponding to male meiosis which occurs earlier than female meiosis (Schneitz et al., 1995). Confocal microscopic examination of the *AtDMC1:NTF/ACT2:BirA* line showed that *NTF* was expressed in the expected cell type. Indeed, we detected GFP-positive male meiocytes during prophase I stage, arguably before the nuclear envelope breakdown (NEBD; **Figure 1**). To purify labeled nuclei from meiocytes, we extracted total nuclei from whole inflorescences with buds at floral stage 9 (Smyth et al., 1990) in the *AtDMC1:NTF/ACT2:BirA* line. Then, the nuclei were incubated

with streptavidin-coated magnetic beads according to INTACT protocols (Deal and Henikoff, 2011; Wang and Deal, 2015). After nucleus isolation, we used a fluorescence microscope to observe the complex DAPI-stained nuclei/beads (**Figure 2**).

### RNA-seq From Isolated Nuclei of the Meiocytes

To obtain the meiotic nuclear transcriptome, RNA sequencing (RNA-seq) was performed downstream of INTACT. RNA extracted from isolated nuclei of meiocytes in three replicates

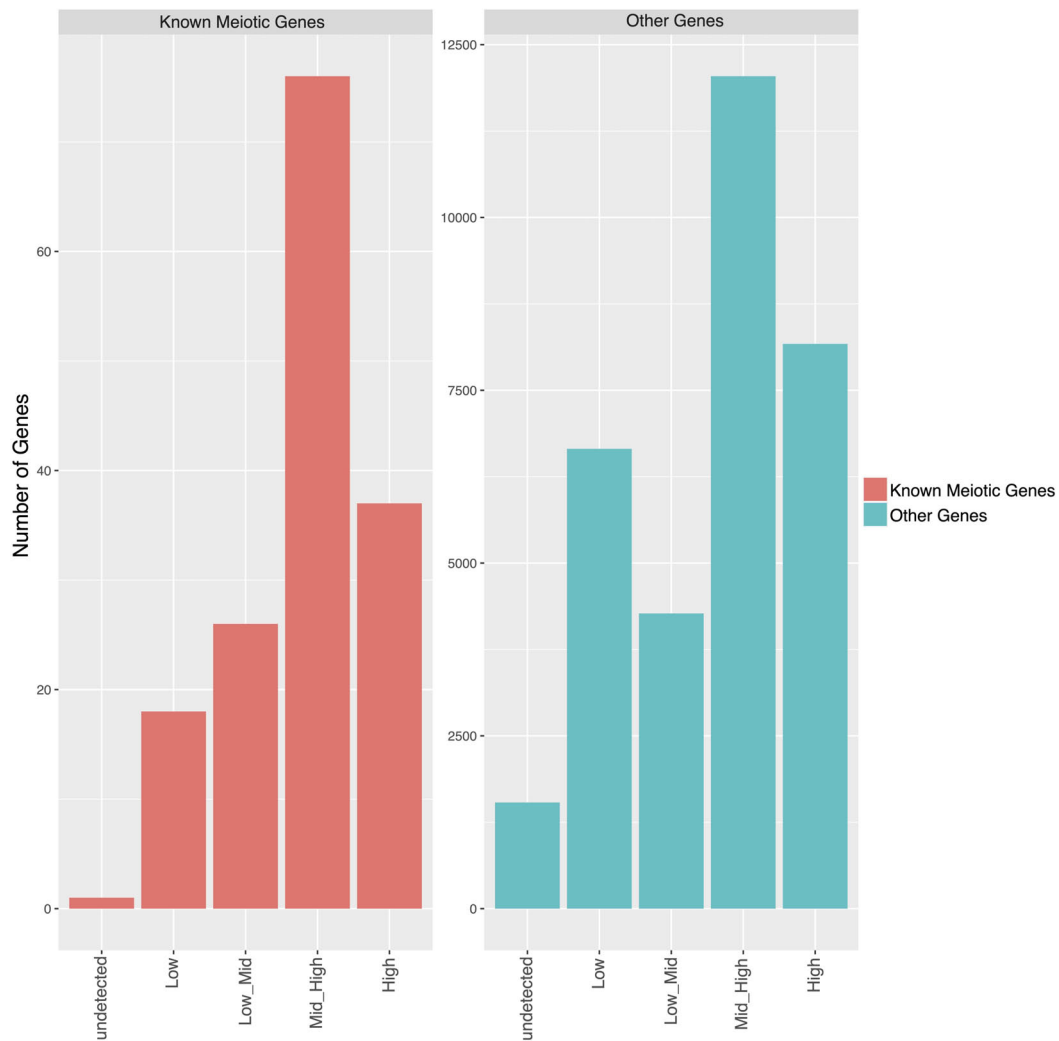
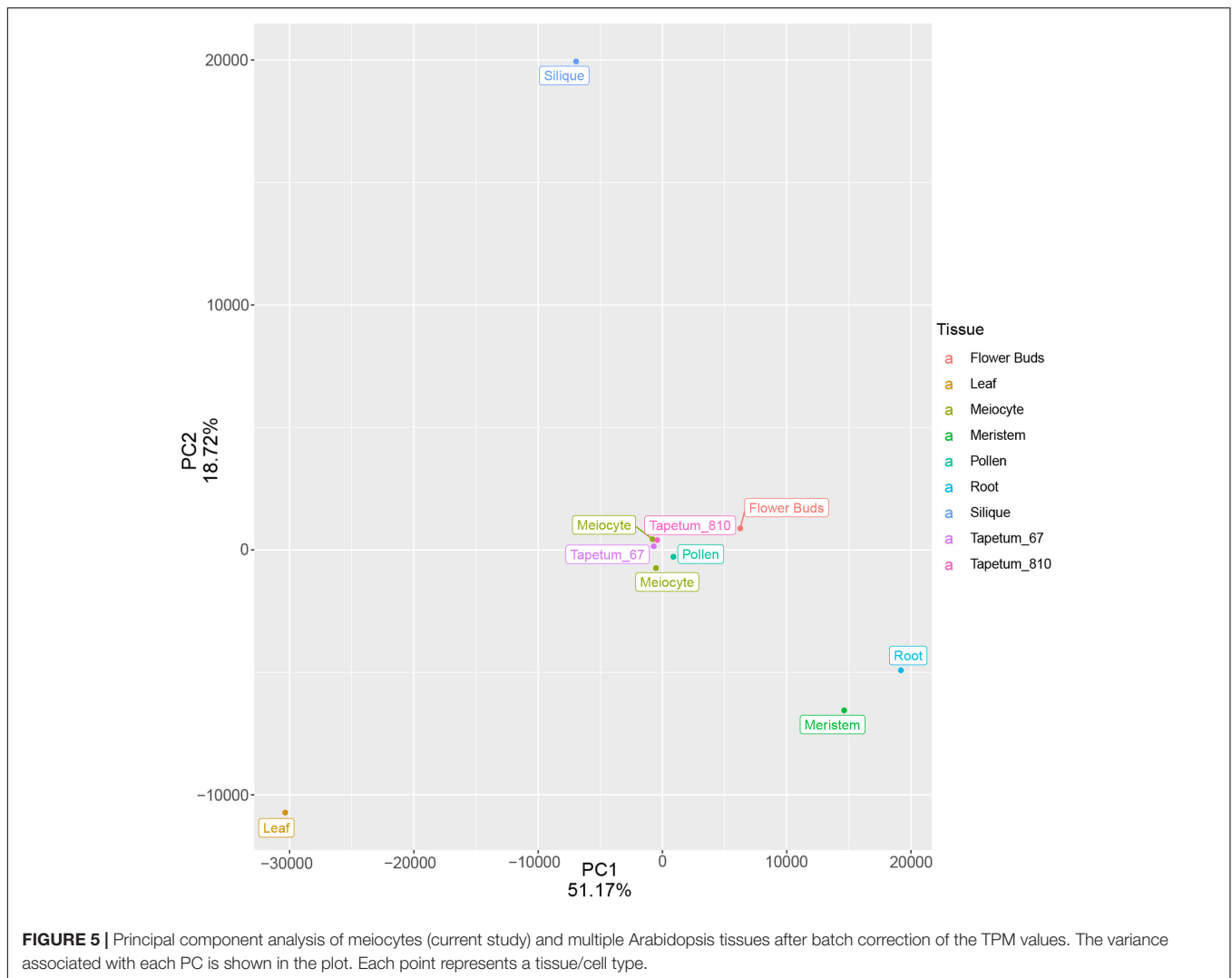


**FIGURE 4** | Bar plot showing the number of genes classified in expression ranges in the meiotic cells. Genes were classified based on their average expression levels using the following criteria: “undetected” if the expression level was 0 in all the replicates, “Low” if  $\log_2$  average TPM  $\leq 1.252$ , “Low\_Mid” if  $\log_2$  average TPM  $> 1.252$  and  $\leq 2.207$ , “Mid\_High” if  $\log_2$  average TPM  $> 2.207$  and  $\leq 4.169$ , and “High” if  $\log_2$  average TPM  $> 4.169$ . Genes were divided into known meiotic genes (left) and other genes (right).

was sequenced by using the Illumina technology following an amplification step. Pearson’s correlation coefficient indicated the reliability of the experiment (**Supplementary Figure 1**). After trimming, an average of 85,927,325 reads per replicate were obtained (**Supplementary Table 5**). About 77% of these reads were mapped onto the Arabidopsis genome (**Supplementary Table 6**). The percentages (calculated as average of the replicates) of the uniquely mapped reads located in known exons, introns, and intergenic regions are 38, 26, and 36%, respectively (**Supplementary Figure 2**). Given the high percentage of reads that mapped to multiple positions (**Supplementary Table 6**), the gene expression, measured as TPM (Transcript Per Million), was calculated by a specific algorithm (Kallisto) which is able to process multiple mapping reads (**Supplementary Table 7**). A frequency ranging between 75.2 and 81.3% of the genes (total no. 32,833) was detected across the replicates

(**Supplementary Figure 3**). Transcript types of each replicate are summarized in **Figure 3** showing the distribution of expression profiles for the different gene classes. Ribosomal RNA appeared the most abundant class whereas lncRNA is the less expressed class. This result is consistent with a recent study in barley in which 65% of the downregulated DEGs were lncRNAs in leptotene/zygotene vs. pre-meiosis comparison (Barakate et al., 2020).

Transcripts were grouped into four classes according to their expression levels from low to high (**Supplementary Figure 4**). GOEA was performed to identify enriched (i.e., over-represented) GO terms associated with the different expression classes (**Supplementary Figures 5A–D**). The most enriched GO terms, such as “DNA demethylation” in the mid/high-expression class and “RNA stabilization” in the high expression class, suggest that these biological processes are particularly relevant to meiosis.



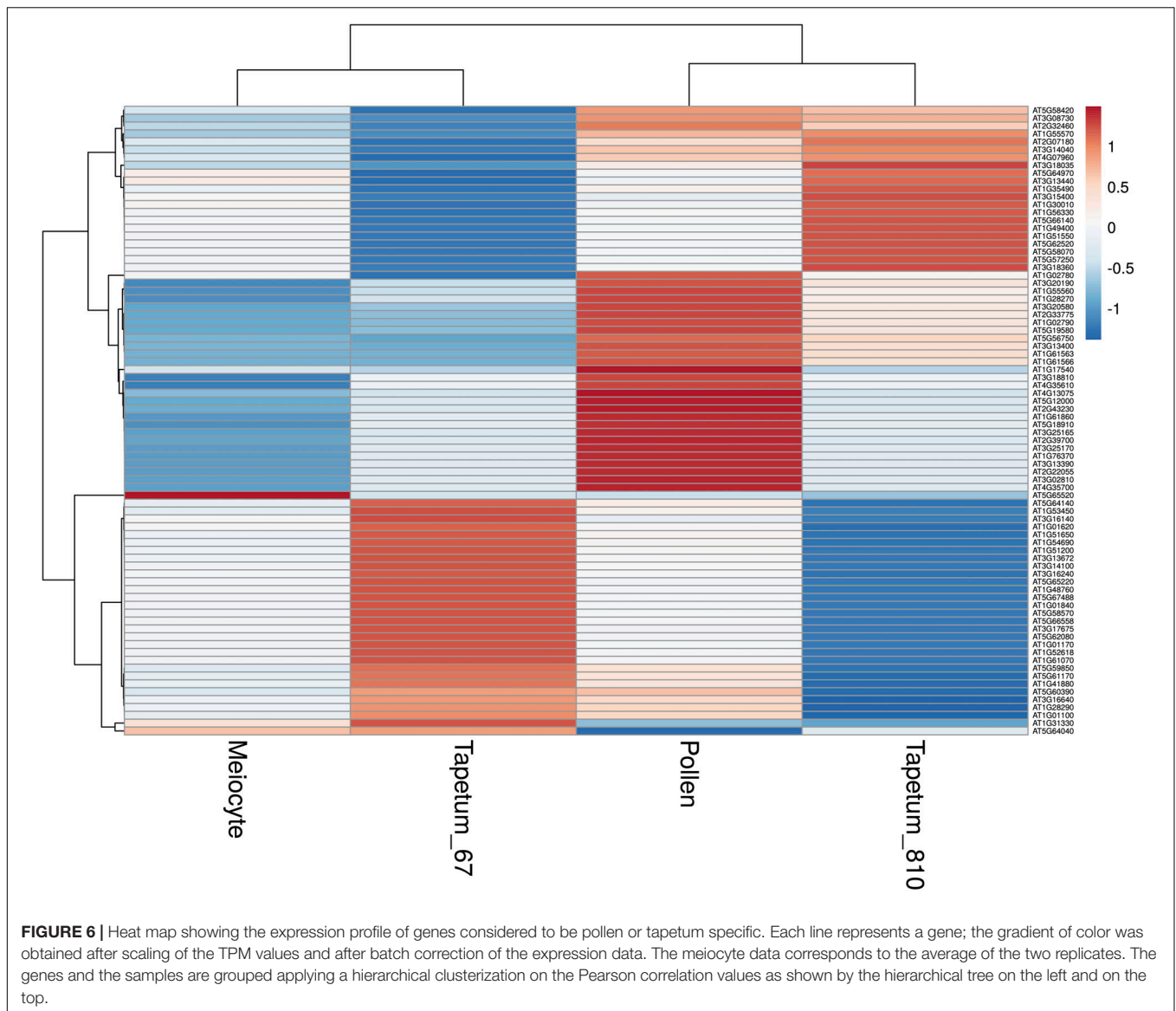
To assess the reliability of our results, we surveyed the genes with documented functions in Arabidopsis meiosis. A list of 197 meiotic genes was implemented using GO terms GO:0051321 (meiotic cell cycle) and GO:0140013 (meiotic nuclear division) (**Supplementary Table 8**). The majority of meiotic genes were distributed in the classes of mid/high and high expression while a small number were in the low-expression class (**Figure 4**). By comparison, this class was the third most represented for the total of transcripts (**Supplementary Figure 4**).

## Transcriptome Comparison Between Male Meiocytes and Other Tissues

To further characterize our meiotic transcriptome, we compared it with publicly available transcriptomic data from other specific tissues and cell types of Arabidopsis. Initially, we planned to compare our RNA-seq data with those from male meiocytes isolated by micromanipulation in Arabidopsis (Chen et al., 2010; Yang et al., 2011) but, unfortunately, these datasets are not available.

Based on the low expression of *AtDMC1* (**Supplementary Figure 6**), we discarded replicate 1 in all the subsequent analyses. Principal component analysis (PCA) performed with meiocytes (current study), meristem, leaf, root, flower buds, tapetum (from two different developmental stages), pollen, and silique revealed that meiocytes clustered close to flower buds, as expected, but also to tapetum and pollen (**Figure 5**). We evaluated the expression profile of genes (list reported in **Supplementary Table 9**) considered to be specific for these two types of cells (Loraine et al., 2013; Li et al., 2017). The heat map revealed expression patterns specific for meiocytes, tapetum, and pollen (**Figure 6**). On the other hand, a hierarchical sample dendrogram showed that meiocyte sample groups together with tapetum 6–7 as well as pollen with tapetum 8–10 equivalent to a later stage.

Afterward, we assessed the overall gene expression of meiotic genes (list reported in **Supplementary Table 8**) and of the other transcripts in meiocytes and multiple tissues (**Figure 7**). The analysis revealed that the median expression value of meiotic genes was higher in isolated meiocytes when compared to the other tissues/cell types with the exception of floral bud

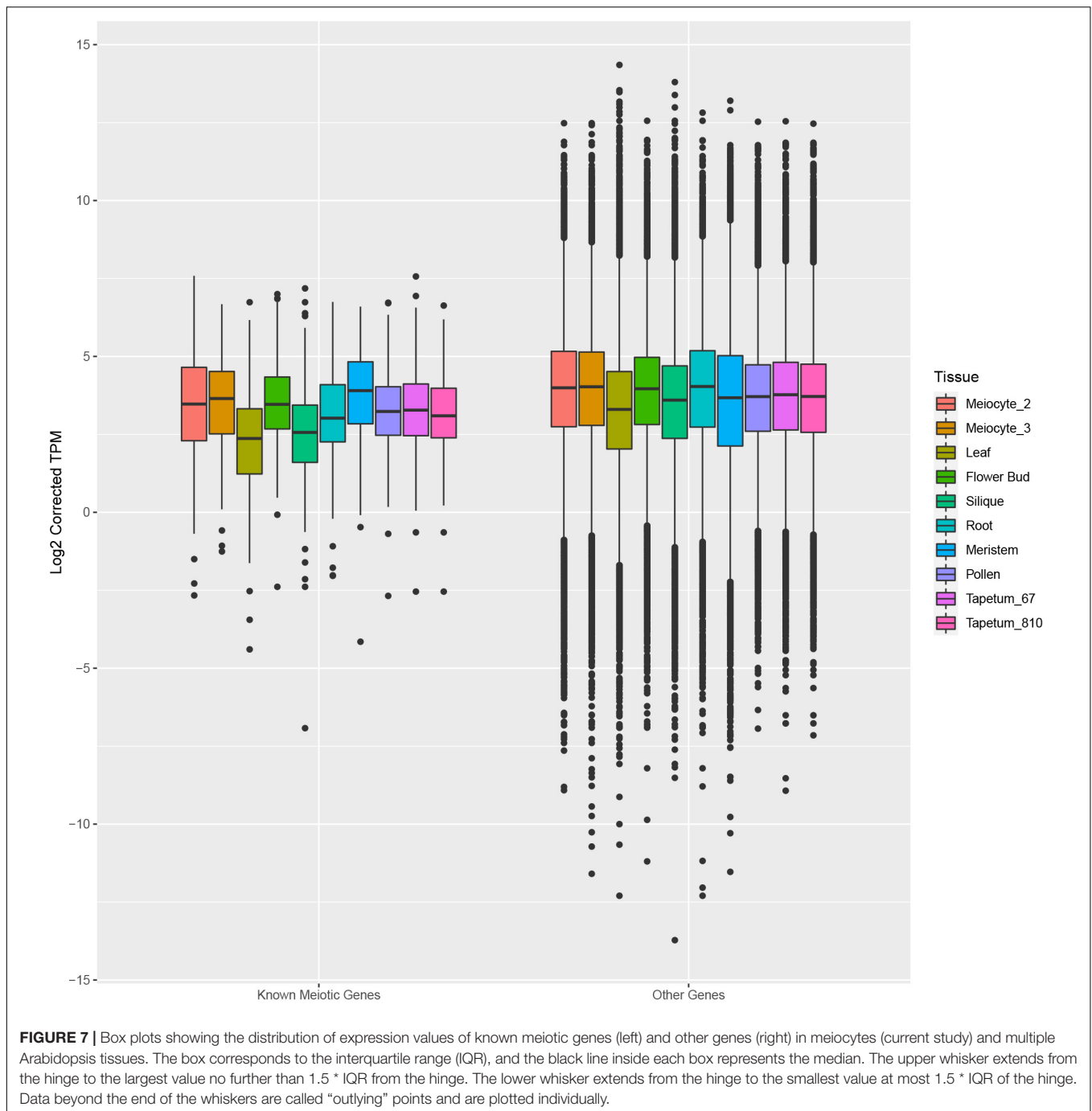


and meristem samples. This result is not surprising since the meioocytes are included in floral buds and they share cell-cycle genes with the meristem. The median expression value of the other transcripts was basically steady across the different tissues (Figure 7). Considering the meiotic gene expression fold changes between meioocytes and the other tissues/cell types, the heat map revealed a pattern in agreement with the above reported analysis (Figure 8 and Supplementary Table 10).

## Meiotic Gene Network

To identify new candidate genes with a meiotic function, we generated a gene expression network based on the genes known to be involved in meiosis (Supplementary Table 8). By selecting the first neighbors of the known meiotic genes, we found 1,503 genes with a total of 7,607 connections (Figure 9 and Supplementary Table 11). The network is characterized by a very large cluster, thereby suggesting that the known meiotic genes

and their neighbors are all highly connected as also indicated by an average degree of 4.95 connections. The most connected genes with 435 and 323 connections have a documented role in meiosis. In particular, FIDGETIN-LIKE-1 INTERACTING PROTEIN (FLIP, AT1G04650) forms a protein complex with FIDGETIN-LIKE-1 (FIGL1) that is conserved from Arabidopsis to human, and it regulates meiotic crossover formation via RAD51 and DMC1 (Fernandes et al., 2018). The other gene, AXR1 (AT1G05180), is involved in the neddylation/rubylation protein modification pathway and TE methylation in meioocytes (Jahns et al., 2014; Christophorou et al., 2020). AXR1 plays a significant role in DNA repair (Martinez-Garcia et al., 2020). Collectively, this finding reinforces the reliability of the analysis performed in this study. New candidates which could play a role in meiosis are two transcription factors (TFs), AT1G06070 and AT1G02220, with 64 and 30 connections, respectively. These two genes belong to the bZIP and NAC TF families,



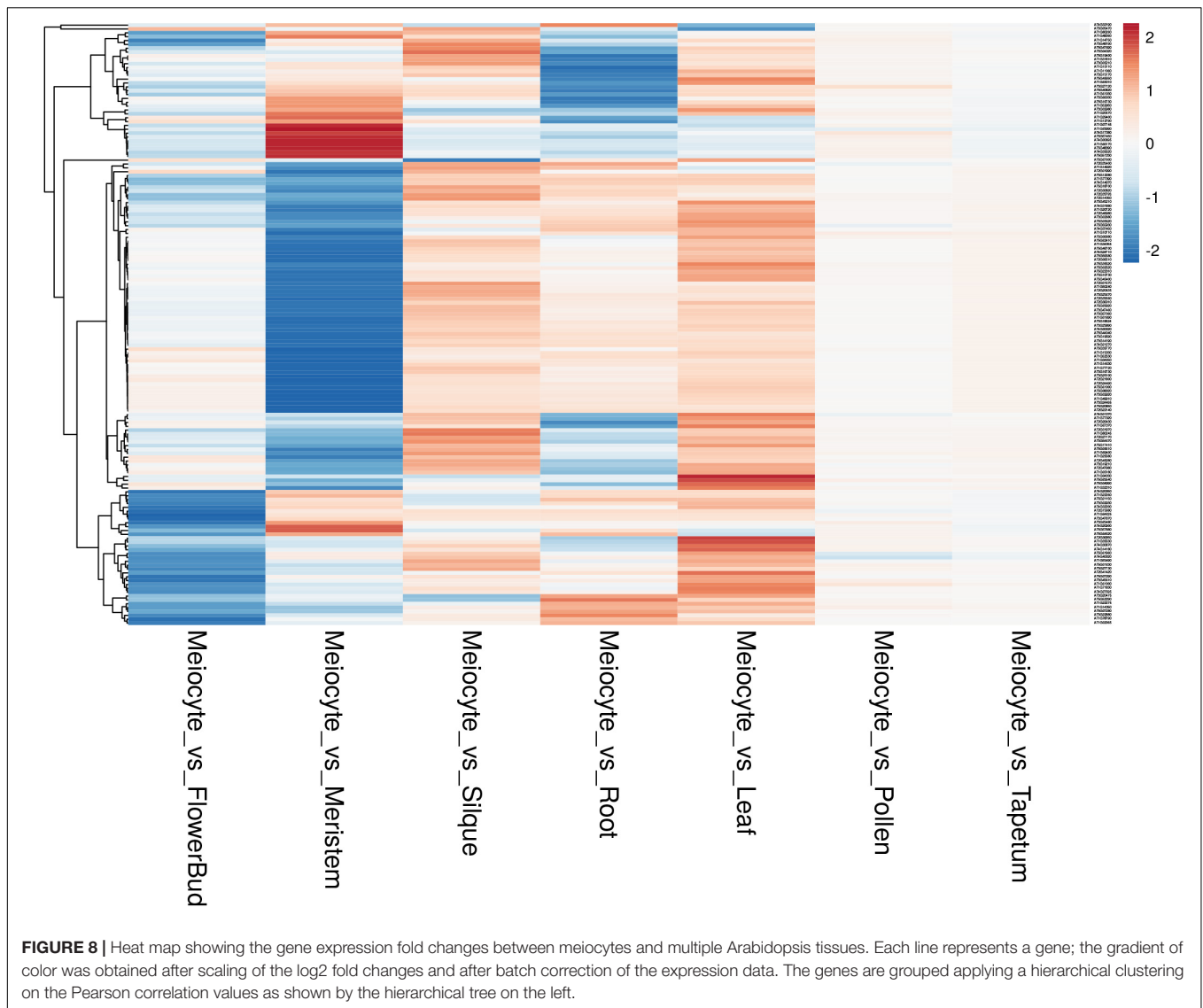
and their function in meiosis has not been documented. Although with less connections than the genes reported above, AT1G04200, described as Dymeclin (DYM, Dyggve–Melchior–Clausen syndrome protein), is an interesting candidate for a possible meiotic function. Indeed, the mouse DYM homolog has a high expression in testis (Yue et al., 2014) and has a proved interaction with FANCD2, a component of the Fanconi anemia DNA repair pathway (Zhang et al., 2017).

A GO analysis performed using the genes identified by the network analysis revealed GO targets associated with

meiotic processes and, particularly, to Meiosis I such as recombination, synapsis, chiasma assembly, and meiotic chromosome segregation (Figure 10 and Supplementary Table 12).

## DISCUSSION

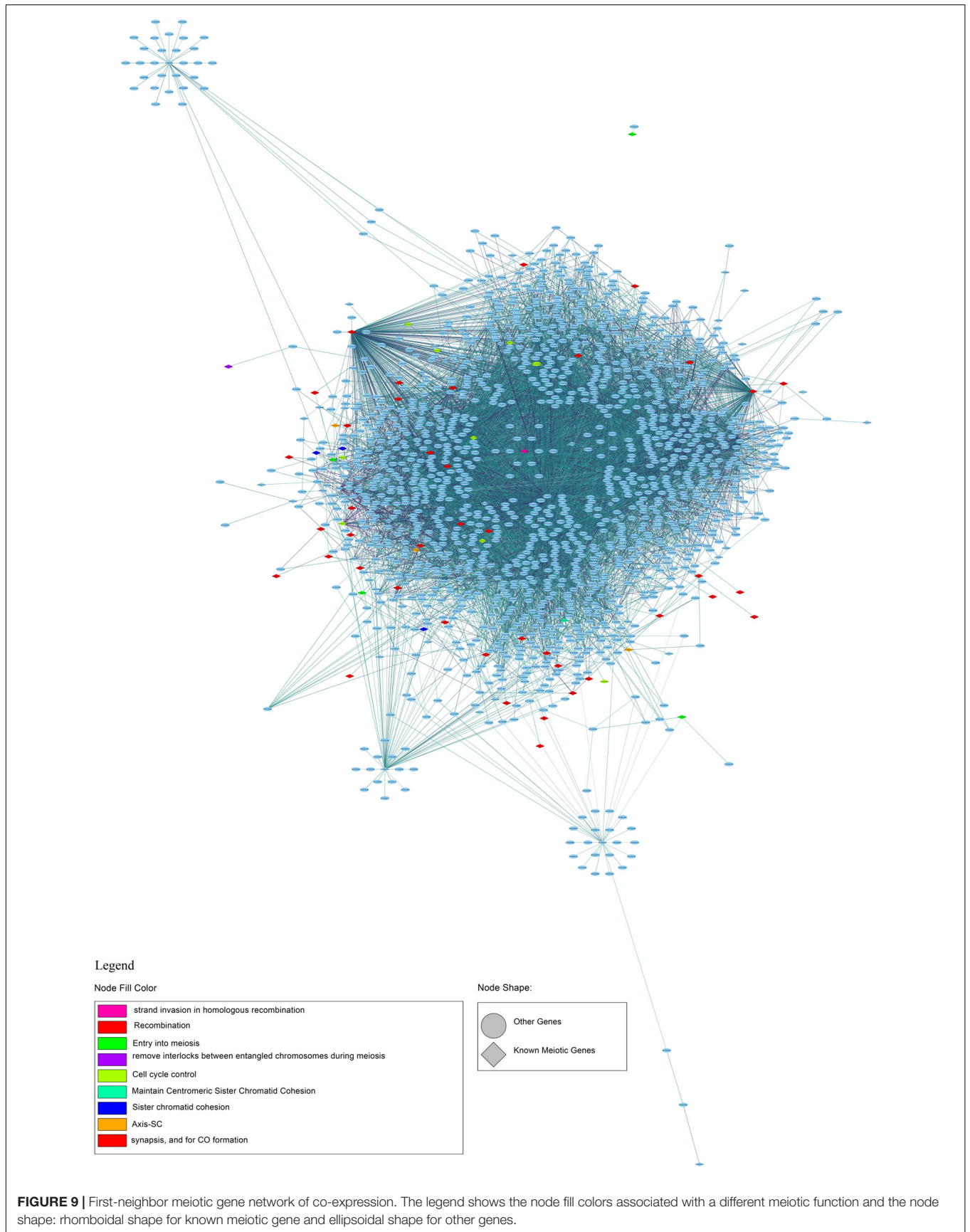
In this work, we reported the application of the INTACT method in meiotic isolation in *A. thaliana*. INTACT entails



the use of a transgene that can be driven by spatially and/or temporally regulated promoters enabling the isolation of nuclei from specific cell types (Deal and Henikoff, 2010). In our experiment, because of a limited number of effective meiotically active promoters available, we employed the established *AtDMC1* promoter widely used in meiotic studies (Li et al., 2012). *AtDMC1* is a recombinase involved in Double Strand Break (DSB) repair and expressed during early prophase I in both male and female meiotic cells in anthers and carpels, respectively (Klimyuk and Jones, 1997; De Muyt et al., 2009). However, *AtDMC1* activity is not restricted only to meiotic cells. Indeed, *AtDMC1* has been observed in embryonic cell culture (Doutriaux et al., 1998) and in young seedlings (Orel et al., 2003). On the other hand, *AtDMC1* was not expressed in the meiocyte's neighboring somatic cells (Klimyuk and Jones, 1997; Li et al., 2012). Our analysis has been restricted to male meiocytes collected from floral buds at a stage corresponding to microsporogenesis (Smyth et al., 1990).

However, it cannot be excluded that female meiocytes also occur in our sample.

Isolation of nuclei tagged in specific cell types allowed us to obtain a nuclear meiotic transcriptome from meiocytes of *A. thaliana* based on RNA-seq data. On average, we detected the expression of about 25,000 genes corresponding to 76% of total genes. Similarly, approximately 22,000 and 24,000 genes were found to be expressed in Arabidopsis male meiocytes isolated in previous studies based on RNA-seq (Chen et al., 2010; Yang et al., 2011). Consistently, 60% or more of all genes in the genome were estimated to be expressed in rice and Arabidopsis male meiocytes (Schmidt et al., 2012). In Arabidopsis, the male meiotic transcriptome shows the largest overlap (approximately 67%) with tissues having cells in active division, including floral buds, anthers, and shoot apex (Yang et al., 2011). The number of reads in our RNA-seq experiment, and particularly the number of uniquely mapped reads, was higher in our study compared to that previously published (56 vs. 33%) (Yang et al., 2011). In addition,





prophase I substages. Apparently, however, the high number of transcripts and the fact that genes involved in later meiotic stages are expressed in our dataset seem to not support our expectations. For instance, the *AtPS1* (*Parallel Spindle 1*, AT1G34355) involved in the orientation of the spindles in Meiosis II (d'Erfurth et al., 2008) was present in the mid-high expression class in our dataset. This finding can be justified by different explanations. First, AtDMC1 could be expressed in other meiotic stages besides prophase I. Second, timing of the gene expression is not strictly associated with timing of the encoded protein function, as evidenced in maize prophase I (Nelms and Walbot, 2019). Finally, the transcriptional basis relevant for meiosis is already set up before its onset, as reported in rice and maize (Tang et al., 2010; Yuan et al., 2018). In the future, other prophase I-expressed genes could be used to build more INTACT lines. For this purpose, we suggest as candidates some meiosis-specific genes with established roles in prophase I identified in mid/high- and high-expression classes of our dataset (**Supplementary Table 13**). These genes exhibit a very low expression in the other tissues (leaf, root, meristem, flower bud, pollen, tapetum, and silique). In addition, they appear to be expressed also in maize at early prophase I as evidenced by the single-cell RNA-seq experiment (Nelms and Walbot, 2019).

The question whether all genes in meiotic transcriptome are essential for meiosis or whether the large number of transcripts is the result of a global de-repression of chromatin during meiosis remains to be answered (Lambing and Heckmann, 2018). Our study evidenced the prevalence of the biological process “DNA demethylation” when we considered the mid/highly expressed genes. Consistently, the upregulation of transposons (TEs) has been reported to be a prominent feature in Arabidopsis male meocytes (Chen et al., 2010; Yang et al., 2011), and it supports the suggestion that DNA methylation decreases at meiosis onset (Kawashima and Berger, 2014). Methylome analysis showed that meocytes have higher CG and CHG methylation but lower CHH methylation in comparison to somatic tissues (Walker et al., 2018). Therefore, it is likely that DNA demethylation engages the CHH context which, on the other hand, is interconnected with TEs. This view is reinforced by the methylome analysis of meocytes in *axr1* mutant (Christophorou et al., 2020). Indeed, this mutation, which affects general DNA methylation in plants, showed a specific increase in meocytes for CHH methylation in TEs. Remarkably, gene expression network analysis performed in our work identified *AXR1* as a relevant hub thereby confirming its important roles in meiosis (Jahns et al., 2014; Christophorou et al., 2020; Martinez-Garcia et al., 2020). Furthermore, DNA

demethylation could have a profound influence on gene expression through TEs (Wang and Baulcombe, 2020). TEs can act *in cis* to affect expression of adjacent genes as observed in male meocytes by Yang et al. (2011). Finally, our co-expression network revealed different gene modules related to meiosis as well as novel candidate genes with a potential meiotic role. The functional analysis of the candidate meiotic genes will contribute to our understanding of meiosis.

## DATA AVAILABILITY STATEMENT

Raw sequencing data obtained by the INTACT experiment was deposited in the Sequence Read Archive (SRA) database of NCBI within the BioProject PRJNA668331.

## AUTHOR CONTRIBUTIONS

LB and PT performed the experiments. PT designed the main experiments. RAC performed the bioinformatics analysis. GC performed the cytological analysis. RP and CL assisted with the experiments. PT, RAC, and GC contributed to the manuscript editing. CC conceived the study and wrote the grant. CC, LB, and FC wrote the manuscript. All authors contributed to the article and approved the submitted version.

## FUNDING

This work was funded by the Epigenomics Flagship Project (EPIGEN) from the Italian Ministry of University and Research (MUR) and the National Research Council of Italy (CNR).

## ACKNOWLEDGMENTS

The authors thank M. Rankenburg for proofreading and R. Nocerino for technical assistance in plant growth condition control.

## SUPPLEMENTARY MATERIAL

The Supplementary Material for this article can be found online at: <https://www.frontiersin.org/articles/10.3389/fpls.2021.638051/full#supplementary-material>

## REFERENCES

- Agrawal, P., Chung, P., Heberlein, U., and Kent, C. (2019). Enabling cell-type-specific behavioral epigenetics in *Drosophila*: a modified high-yield INTACT method reveals the impact of social environment on the epigenetic landscape in dopaminergic neurons. *BMC Biol.* 17:30. doi: 10.1186/s12915-019-0646-4
- Amin, N. M., Greco, T. M., Kuchenbrod, L. M., Rigney, M. M., Wallingford, J. B., et al. (2014). Proteomic profiling of cardiac tissue by isolation of nuclei tagged in specific cell types (INTACT). *Development* 141, 962–973. doi: 10.1242/dev.098327
- An, Y.-Q., McDowell, J. M., Huang, S., McKinney, E. C., Chambliss, S., and Meagher, R. B. (1996). Strong, constitutive expression of the *Arabidopsis* ACT2/ACT8 actin subclass in vegetative tissues. *Plant J.* 10, 107–121. doi: 10.1046/j.1365-313x.1996.10010107.x
- Barakate, A., Orr, J., Schreiber, M., Colas, I., Lewandowska, D., McCallum, N., et al. (2020). Time-resolved transcriptome of barley anthers and meocytes reveals robust and largely stable gene expression changes at meiosis entry. *bioRxiv* [preprint] doi: 10.1101/2020.04.20.051425
- Barra, L., Aiese-Cigliano, R., Cremona, G., De Luca, P., Zoppoli, P., Bressan, R. A., et al. (2012). Transcription profiling of laser microdissected microsporocytes

- in an *Arabidopsis mutant* (Atmcc1) with enhanced histone acetylation. *J. Plant Biol.* 55, 281–289. doi: 10.1007/s12374-011-0268-z
- Beckett, D., Kovaleva, E., and Schatz, P. J. (1999). A minimal peptide substrate in biotin holoenzyme synthetase-catalyzed biotinylation. *Protein Sci.* 8, 921–929. doi: 10.1110/ps.8.4.921
- Bushnell, B., Rood, J., and Singer, E. (2017). BBMerge – Accurate paired shotgun read merging via overlap. *PLoS One* 12:e0185056. doi: 10.1371/journal.pone.0185056
- Chen, C., Farmer, A., Langley, R., Mudge, J., Crow, J., May, G., et al. (2010). Meiosis-specific gene discovery in plants: RNA-Seq applied to isolated *Arabidopsis* male meiocytes. *BMC Plant Biol.* 10:280. doi: 10.1186/1471-2229-10-280
- Cheng, C. Y., Krishnakumar, V., Chan, A. P., Thibaud-Nissen, F., Schobel, S., and Town, C. D. (2016). Araport11: a complete reannotation of the *Arabidopsis thaliana* reference genome. *Plant J.* 89, 789–804. doi: 10.1111/tpj.13415
- Christophorou, N., She, W., Long, J., Hurel, A., Beaubiat, S., Idir, Y., et al. (2020). AXR1 affects DNA methylation independently of its role in regulating meiotic crossover localization. *PLoS Genet.* 16:e1008894. doi: 10.1371/journal.pgen.1008894
- Clough, S. J., and Bent, A. F. (1998). Floral dip: a simplified method for *Agrobacterium*-mediated transformation of *Arabidopsis thaliana*. *Plant J.* 16, 735–743. doi: 10.1046/j.1365-313x.1998.00343.x
- De Muyt, A., Pereira, L., Vezon, D., Chelysheva, L., Gendrot, G., Chambon, A., et al. (2009). A high throughput genetic screen identifies new early meiotic recombination functions in *Arabidopsis thaliana*. *PLoS Genet.* 5:e1000654. doi: 10.1371/journal.pgen.1000654
- De Storme, N., and Geelen, D. (2014). The impact of environmental stress on male reproductive development in plants: biological processes and molecular mechanisms. *Plant Cell Environ.* 37, 1–18. doi: 10.1111/pce.12142
- Deal, R. B., and Henikoff, S. (2010). A simple method for gene expression and chromatin profiling of individual cell types within a tissue. *Dev. Cell* 18, 1030–1040. doi: 10.1016/j.devcel.2010.05.013
- Deal, R. B., and Henikoff, S. (2011). The INTACT method for cell type-specific gene expression and chromatin profiling in *Arabidopsis thaliana*. *Nat. Protoc.* 6, 56–68. doi: 10.1038/nprot.2010.175
- Del Toro-De León, G., and Köhler, C. (2019). Endosperm-specific transcriptome analysis by applying the INTACT system. *Plant Reprod.* 32, 55–61. doi: 10.1007/s00497-018-00356-3
- d'Erfurth, I., Jolivet, S., Froger, N., Catrice, O., Novatchkova, M., Simon, M., et al. (2008). Mutations in AtPS1 (*Arabidopsis thaliana* parallel spindle 1) lead to the production of diploid pollen grains. *PLoS Genet.* 4:e1000274. doi: 10.1371/journal.pgen.1000274
- Doutriaux, M. P., Couteau, F., Bergounioux, C., and White, C. (1998). Isolation and characterisation of the RAD51 and DMC1 homologs from *Arabidopsis thaliana*. *Mol. General Genet.* 257, 283–291. doi: 10.1007/s004380050649
- Dubowicz-Shulze, S., and Chen, C. (2014). The meiotic transcriptome architecture of plants. *Front. Plant Sci.* 5:220. doi: 10.3389/fpls.2014.00220
- Fernandes, J. B., Duhamel, M., Seguela-Arnaud, M., Froger, N., Girard, C., Choinard, S., et al. (2018). FIGL1 and its novel partner FLIP form a conserved complex that regulates homologous recombination. *PLoS Genet.* 14:e1007317. doi: 10.1371/journal.pgen.1007317
- Jahns, M. T., Vezon, D., Chambon, A., Pereira, L., Falque, M., Martin, O. C., et al. (2014). Crossover localisation is regulated by the neddylation posttranslational regulatory pathway. *PLoS Biol.* 12:e1001930. doi: 10.1371/journal.pbio.1001930
- Kawashima, T., and Berger, F. (2014). Epigenetic reprogramming in plant sexual reproduction. *Nat. Rev. Genet.* 15, 613–624. doi: 10.1038/nrg3685
- Klimyuk, V. I., and Jones, J. D. (1997). AtDMC1, the *Arabidopsis* homologue of the yeast DMC1 gene: characterization, transposon-induced allelic variation and meiosis-associated expression. *Plant J.* 11, 1–14. doi: 10.1046/j.1365-313x.1997.11010001.x
- Lambing, C., and Heckmann, S. (2018). Tackling plant meiosis: from model research to crop improvement. *Front. Plant Sci.* 9:829. doi: 10.3389/fpls.2018.00829
- Li, D.-D., Xue, J.-S., Zhu, J., and Yang, Z.-N. (2017). Gene regulatory network for tapetum development in *Arabidopsis thaliana*. *Front. Plant Sci.* 8:1559. doi: 10.3389/fpls.2017.01559
- Li, J., Farmer, A. D., Lindquist, I. E., Dukowicz-Schulze, S., Mudge, J., Li, T., et al. (2012). Characterization of a set of novel meiotically-active promoters in *Arabidopsis*. *BMC Plant Biol.* 12:104. doi: 10.1186/1471-2229-12-104
- Libeau, P., Durandet, M., Granier, F., Marquis, C., Berthome, R., Renou, J. P., et al. (2011). Gene expression profiling of *Arabidopsis* meiocytes. *Plant Biol.* 13, 784–793. doi: 10.1111/j.1438-8677.2010.00435.x
- Loraine, A. E., McCormick, S., Estrada, A., Patel, K., and Qin, P. (2013). RNA-seq of *Arabidopsis* pollen uncovers novel transcription and alternative splicing. *Plant Physiol.* 162, 1092–1109. doi: 10.1104/pp.112.211441
- Martinez-Garcia, M., Fernández-Jiménez, N., Santos, J. L., and Pradillo, M. (2020). Duplication and divergence: new insights into AXR1 and AXL functions in DNA repair and meiosis. *Sci. Rep.* 10:8860. doi: 10.1038/s41598-020-65734-2
- Mercier, R., Mézard, C., Jenczewski, E., Macaisn, N., and Grelon, M. (2015). The molecular biology of meiosis in plants. *Annu. Rev. Plant Biol.* 66, 297–327. doi: 10.1146/annurev-arplant-050213-035923
- Metsalu, T., and Vilo, J. (2015). ClustVis: a web tool for visualizing clustering of multivariate data using principal component analysis and heatmap. *Nucleic Acids Res.* 43, W566–W570. doi: 10.1093/nar/gkv468
- Murashige, T., and Skoog, F. (1962). A revised medium for rapid growth and bio-assays with tobacco tissue cultures. *Physiol. Plantarum* 15, 473–497. doi: 10.1111/j.1399-3054.1962.tb08052.x
- Nelms, B., and Walbot, V. (2019). Defining the developmental program leading to meiosis in maize. *Science* 364, 52–56. doi: 10.1126/science.aav6428
- Okonechnikov, K., Conesa, A., and García-Alcalde, F. (2016). Qualimap 2: advanced multi-sample quality control for high-throughput sequencing data. *Bioinformatics* 32, 292–294. doi: 10.1093/bioinformatics/btv566
- Orel, N., Kyryk, A., and Puchta, H. (2003). Different pathways of homologous recombination are used for the repair of double-strand breaks within tandemly arranged sequences in the plant genome. *Plant J.* 35, 604–612. doi: 10.1046/j.1365-313X.2003.01832.x
- Palovaara, J., Saiga, S., Wendrich, J. R., Wout Hofland, N., Schayck, J. P., Hater, F., et al. (2017). Transcriptome dynamics revealed by a gene expression atlas of the early *Arabidopsis* embryo. *Nat. Plants* 3, 894–904. doi: 10.1038/s41477-017-0035-3
- Parry, M., Rosenzweig, C., Iglesias, A., Fischer, G., and Livermore, M. (1999). Climate change and world food security: a new assessment. *Global Environ. Chang.* 9, S51–S67. doi: 10.1016/S0959-3780(99)00018-7
- Pradillo, M., Evans, D., and Graumann, K. (2019). The nuclear envelope in higher plant mitosis and meiosis. *Nucleus* 10, 55–66. doi: 10.1080/19491034.2019.1587277
- Reynoso, M. A., Pauluzzi, G. C., Kajala, K., Cabanlit, S., Velasco, J., Bazin, J., et al. (2018). Nuclear transcriptomes at high resolution using retooled INTACT. *Plant Physiol.* 176, 270–281. doi: 10.1104/pp.17.00688
- Rose, A., and Meier, I. (2001). A domain unique to plant RanGAP is responsible for its targeting to the plant nuclear rim. *Proc. Natl. Acad. Sci. U S A.* 26, 15377–15382. doi: 10.1073/pnas.261459698
- Sales, G., and Romualdi, C. (2011). Parmigen—a parallel R package for mutual information estimation and gene network reconstruction. *Bioinformatics* 13, 1876–1877. doi: 10.1093/bioinformatics/btr274
- Schmidt, A., Schmid, M. W., and Grossniklaus, U. (2012). Analysis of plant germline development by high-throughput RNA profiling: technical advances and new insights. *Plant J.* 70, 18–29. doi: 10.1111/j.1365-313X.2012.04897
- Schmidt, A., Wuest, S. E., Vijverberg, K., Baroux, C., Kleen, D., and Grossniklaus, U. (2011). Transcriptome analysis of the *Arabidopsis* megaspore mother cell uncovers the importance of RNA helicases for plant germline development. *PLoS Biol.* 9:e1001155. doi: 10.1371/journal.pbio.1001155
- Schneitz, K., Hulskamp, M., and Pruitt, R. E. (1995). Wild type ovule development in *Arabidopsis thaliana* - a light microscope study of cleared whole mount tissue. *Plant J.* 7, 731–749. doi: 10.1046/j.1365-313X.1995.07050731.x
- Si, W., Yuan, Y., Huang, J., Zhang, X., Zhang, Y., Zhang, Y., et al. (2015). Widely distributed hot and cold spots in meiotic recombination as shown by the sequencing of rice F2 plants. *New Phytol.* 206, 1491–1502. doi: 10.1111/nph.13319
- Smyth, D. R., Bowman, J. L., and Meyerowitz, E. M. (1990). Early flower development in *Arabidopsis*. *Plant Cell* 8, 755–767. doi: 10.1105/tpc.2.8.755
- Soneson, C., Love, M. I., and Robinson, M. D. (2016). Differential analyses for RNA-seq: transcript-level estimates improve gene-level inferences. *F1000 Research* 4, 1521–1531. doi: 10.12688/f1000research.7563.2

- Song, Y., Milon, B., Ott, S., Zhao, X., Sadzewicz, L., Shetty, A., et al. (2018). A comparative analysis of library prep approaches for sequencing low input transcriptome samples. *BMC Genomics* 19:696. doi: 10.1186/s12864-018-5066-2
- Tang, X., Zhang, Z. Y., Zhang, W. J., Zhao, X. M., Li, X., Zhang, D., et al. (2010). Global gene profiling of laser-captured pollen mother cells indicates molecular pathways and gene subfamilies involved in rice meiosis. *Plant Physiol.* 154, 1855–1870. doi: 10.1104/pp.110.161661
- Tarazona, S., Furió-Tarí, P., Turrà, D., Di Pietro, A., Nueda, M. J., Ferrer, A., et al. (2015). Data quality aware analysis of differential expression in RNA-seq with NOISeq R/Bioc package. *Nucleic Acids Res.* 43:e140. doi: 10.1093/nar/gkv711
- Tian, T., Liu, Y., Yan, H., You, Q., Yi, X., Du, Z., et al. (2017). AgriGO v2.0: a GO analysis toolkit for the agricultural community, 2017 update. *Nucleic Acids Res.* 45, W122–W129. doi: 10.1093/nar/gkx382
- Walker, J., Gao, H., Zhang, J., Aldridge, B., Vickers, M., Higgins, J. D., et al. (2018). Sexual-lineage-specific DNA methylation regulates meiosis in *Arabidopsis*. *Nat. Genet.* 50, 130–137. doi: 10.1038/s41588-017-0008-5
- Wang, D., and Deal, R. B. (2015). Epigenome profiling of specific plant cell types using a streamlined INTACT protocol and ChIP-seq. *Methods Mol. Biol.* 1284, 3–25. doi: 10.1007/978-1-4939-2444-8\_1
- Wang, Z., and Baulcombe, D. C. (2020). Transposon age and non-CG methylation. *Nat. Commun.* 11, 1221–1229. doi: 10.1038/s41467-020-14995-6
- Yang, H., Pingli, Lu, P., Wang, Y., and Ma, H. (2011). The transcriptome landscape of *Arabidopsis* male meiocytes from high-throughput sequencing: the complexity and evolution of the meiotic process. *Plant J.* 65, 503–516. doi: 10.1111/j.1365-313X.2010.04439.x
- Yuan, T. L., Huang, W. J., He, J., Zhang, D., and Tang, W. H. (2018). Stage-Specific gene profiling of germinal cells helps delineate the mitosis/meiosis transition. *Plant Physiol.* 176, 1610–1626. doi: 10.1104/pp.17.01483
- Yue, F., Cheng, Y., Breschi, A., Vierstra, J., Wu, W., Ryba, T., et al. (2014). A comparative encyclopedia of DNA elements in the mouse genome. *Nature* 515, 355–364. doi: 10.1038/nature13992
- Zhang, T., Du, W., Wilson, A. F., Namekawa, S. H., Andreassen, P.R., Meetei, A. R., et al. (2017). Fancd2 *in vivo* interaction network reveals a non-canonical role in mitochondrial function. *Sci. Rep.* 7, 45626–45636. doi: 10.1038/srep45626

**Conflict of Interest:** RAC was employed by company Sequentia Biotech SL.

The remaining authors declare that the research was conducted in the absence of any commercial or financial relationships that could be construed as a potential conflict of interest.

Copyright © 2021 Barra, Termolino, Aiese Cigliano, Cremona, Paparo, Lanzillo, Consiglio and Conicella. This is an open-access article distributed under the terms of the Creative Commons Attribution License (CC BY). The use, distribution or reproduction in other forums is permitted, provided the original author(s) and the copyright owner(s) are credited and that the original publication in this journal is cited, in accordance with accepted academic practice. No use, distribution or reproduction is permitted which does not comply with these terms.